A Novel Method for the Remote Detection of Debonding in FRP-strengthened Concrete: Acoustic-Laser Vibrometry

Justin G. Chen[1], Robert W. Haupt[2], Oral Büyüköztürk[1]
[1]Department of Civil and Environmental Engineering, MIT
77 Massachusetts Ave., Cambridge, MA 02139
(617) 253-7186, obuyuk@mit.edu

[2]MIT Lincoln Laboratory
244 Wood Street, Lexington, MA 02421

INTRODUCTION

Fiber-reinforced polymer (FRP) strengthening and retrofitting of concrete structural elements in civil infrastructure systems has become increasingly popular since the 1990s, especially in areas where earthquakes are prevalent [1,2]. When defects such as voids or delamination occur in these FRP-reinforced concrete elements at the FRP-concrete interface, the FRP obscures the defect such that visual detection may not be possible. Detection of such defects is especially important in the case where FRP has been retrofitted to previously damaged structures and further damage is a distinct possibility.

Current Methods

Most currently available non-destructive testing (NDT) methods rely on physical contact, however a robust standoff method for measuring such damage does not exist; an NDT method that is capable of remotely assessing damage is urgently needed. Currently available and recently studied NDT technologies for FRP retrofitted concrete include elastic wave, ultrasound, x-ray, and radar methods [3,4]. These methods all share the disadvantage of requiring either contact or close proximity of equipment with the specimen under test. Standoff methods of damage detection have numerous advantages over contact measurement methods since they allow for measurement of damage in locations that are physically difficult to access, such as high above the ground or over water. Also, measurements covering a large area are simpler since the equipment can simply be swept along a surface or reaimed to measure a different location. In order to make standoff measurements of FRP-retrofitted concrete, a novel approach called the acoustic-laser vibrometry method is used, which exploits the fact that areas where the FRP has debonded from concrete will vibrate in response to an acoustic excitation like a drum head.

METHODOLOGY

Laser vibrometry has the ability to measure the surface movement of objects from relatively large distances. To first order, measurements of velocity are only limited by the laser power available and line of sight [5]. With the advent of commercial off-the-shelf laser vibrometers, they are being used in various research applications in non-destructive testing such as brake rotors and engine manifolds among other things in the automotive industry [6], ripeness of fruit [7], land mine detection [8,9], bubbles in paint coatings [10], and damage in composite materials [11,12].

A laser vibrometer and an acoustic excitation are combined to form a standoff system that is capable of locating and measuring defects in FRP-retrofitted concrete. This is called the acoustic-laser vibrometry method, as illustrated in Figure 1. When excited by the acoustic source, defective areas of FRP will vibrate with an amplitude greater than that of intact areas. The surface vibration field of the specimen is measured, and depending on the response frequency and areas where the response is exaggerated, defects can be located. It is a powerful technique that allows for non-contact measurement and can be made into a relatively compact and portable system.

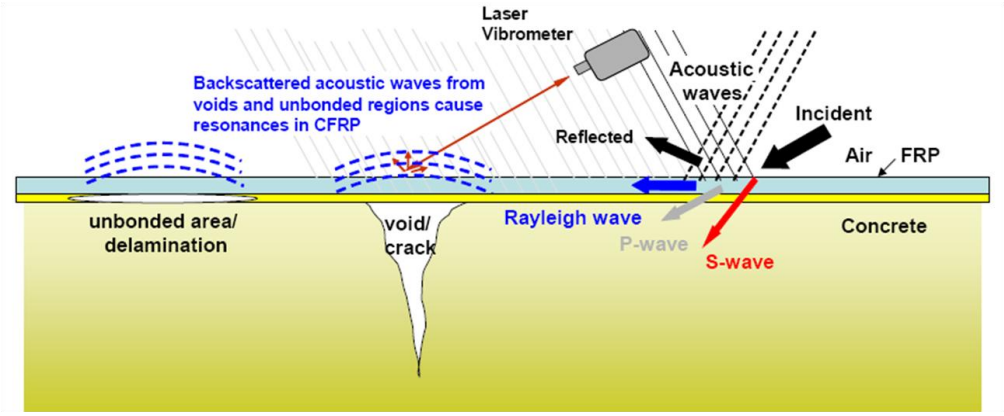

Figure 1: Illustration of the acoustic-laser vibrometry method

Theory

The general theory that the acoustic-laser vibrometry system works on, is that air pressure from sound waves will induce vibrations in damaged areas of FRP greater than that of surrounding intact areas. The debonding or delamination of FRP allows it to freely vibrate on the surface like a drum head, while in the case of intact material, epoxy firmly bonds the FRP to the concrete. The amplitude of surface vibration is measured with a laser vibrometer that can be aimed to allow us locate the defect with approximately millimeter accuracy. When excited by a broadband acoustic source, the defect will exhibit specific resonant frequencies that identify the size and geometry of the defect. A mathematical model for the defect is formulated to calculate an estimation for the resonant frequencies given the size and geometry of the defect.

Plate Theory

To model a defect where the FRP has delaminated from the concrete in a certain area, consider a simplified mathematical model: a square clamped plate. Even though FRP is a directional material, for simplicity it is assumed to be isotropic. Also, the air beneath the plate, which is much less dense and less stiff than the FRP, is assumed to have a negligible effect on the resonant frequencies of the plate. The boundary where the FRP is bonded to the concrete is assumed to be a clamped boundary condition. The plate equation that governs this defect is as follows [13,14]:

$$D\nabla^4 w + \rho h \frac{\partial^2 w}{\partial t^2} = 0$$

where $D = \frac{Eh^3}{12(1-\nu^2)}$ = flexural rigidity of the plate, E = Young's modulus, h = thickness of the plate, ν = Poisson's ratio, ρ = density of the material, and $w = w(x, y, t)$ transverse displacement of the plate as a function of spatial variables x, y and time t. From this equation, the resonant frequencies of the plate are determined by the equation:

$$f = \frac{\lambda}{2\pi a^2}\sqrt{\frac{D}{\rho h}}$$

where λ = a frequency parameter that depends on the resonant mode, geometry, and boundary conditions of the plate, a = side length of the square plate, and f = resonant frequency. These equations can be used to calculate the expected resonant frequency of the different vibrational modes of the plate, assuming an isotropic material. Fiberglass is not an isotropic material, therefore this method is only reasonable for giving an estimate of the fundamental resonant frequency. Using the following material property values, a table of resonant frequencies are calculated, as shown in Table 1. If the material properties of the FRP system are known, such as the Young's modulus, Poisson's ratio, density, and thickness of the FRP plate, and an assumption can be made regarding the geometry and boundary condition of the defect to determine λ, a characteristic size of the defect can be back-calculated from the measured resonant frequency of the defect.

Table 1: Material Properties and calculated resonant frequencies

Material Properties of FRP			Calculated Resonant Frequencies	
Defect side length	0.0762 m		Mode	Frequency (Hz)
Young's modulus	20.9 GPa		1, 1	1288
Poisson's ratio	0.2		2, 1	2626
Density	1800 kg/m^3		2, 2	3872
Thickness	1.3 mm		3, 1	4719

Experimental System

The experimental setup involved a laser vibrometer, a loudspeaker, the sample under test, and an analog to digital converter and associated data collection equipment. The arrangement of the equipment was such that the laser vibrometer measures the sample normal to its surface to avoid any errors in the vibration magnitude. The theory predicts a flexural wave in the defect, so maximum amplitude was measured normal to the surface. The speaker was placed approximately one meter away from the sample and slightly off the line of sight of the laser vibrometer to avoid obstruction of the laser. The laser vibrometer is placed about three meters away from the sample, a distance close enough to maintain good signal strength, while avoiding acoustic coupling from the speaker into the vibrometer. Retroreflective tape was used on the target to ensure a good return signal from the target for the laser vibrometer.

Test Specimen

In order to test the system a FRP-retrofitted concrete panel was fabricated with a created defect as shown in figure 6, designated as "FRP-P2". It consists of a concrete panel that is 12” by 12” by 4” and has three reinforcing bars inside. During the casting process of the panel, a 3" by 3" by 0.2" foam piece was placed in the mold to create an air void. Then a wet layup procedure was used to bond the FRP to the panel, with the air void resulting in a defect under the FRP. The specimen and measurement locations are shown in Figure 2.

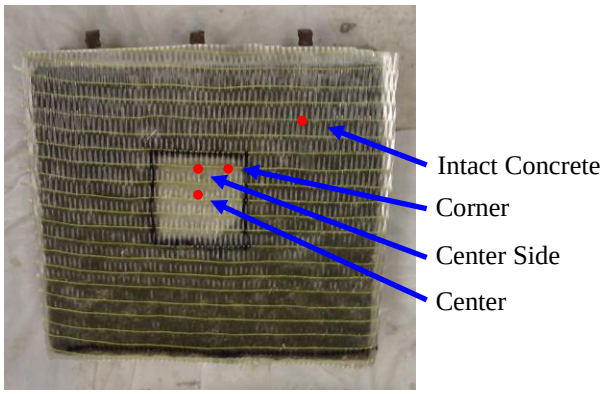

Figure 2: FRP-bonded reinforced concrete panel, delamination defect, FRP-P2

Measurement Procedure

In order to determine the frequency response of the defect, measurements were made with the laser vibrometer while a 0-20kHz frequency sweep was played on the loudspeaker. The frequency sweep excites the test specimen over a wide range of frequencies, so that any resonant frequency belonging to a defect will be excited and the corresponding increase in vibration amplitude will be measured. Different waveforms, such as white noise, can also be used to excite the specimen.

RESULTS

Preliminarily, test specimens were measured in 4 locations, over the center of the defect, side of the defect, corner of the defect, and over intact material. A frequency sweep was used to excite the test specimen, and the vibration amplitudes were scaled, by multiplying by the square root of frequency sweep length times frequency bandwidth, to

match the equivalent constant tone vibration amplitude. This was to determine the vibration amplitude frequency dependence at different locations and the responses are plotted in Figure 3.

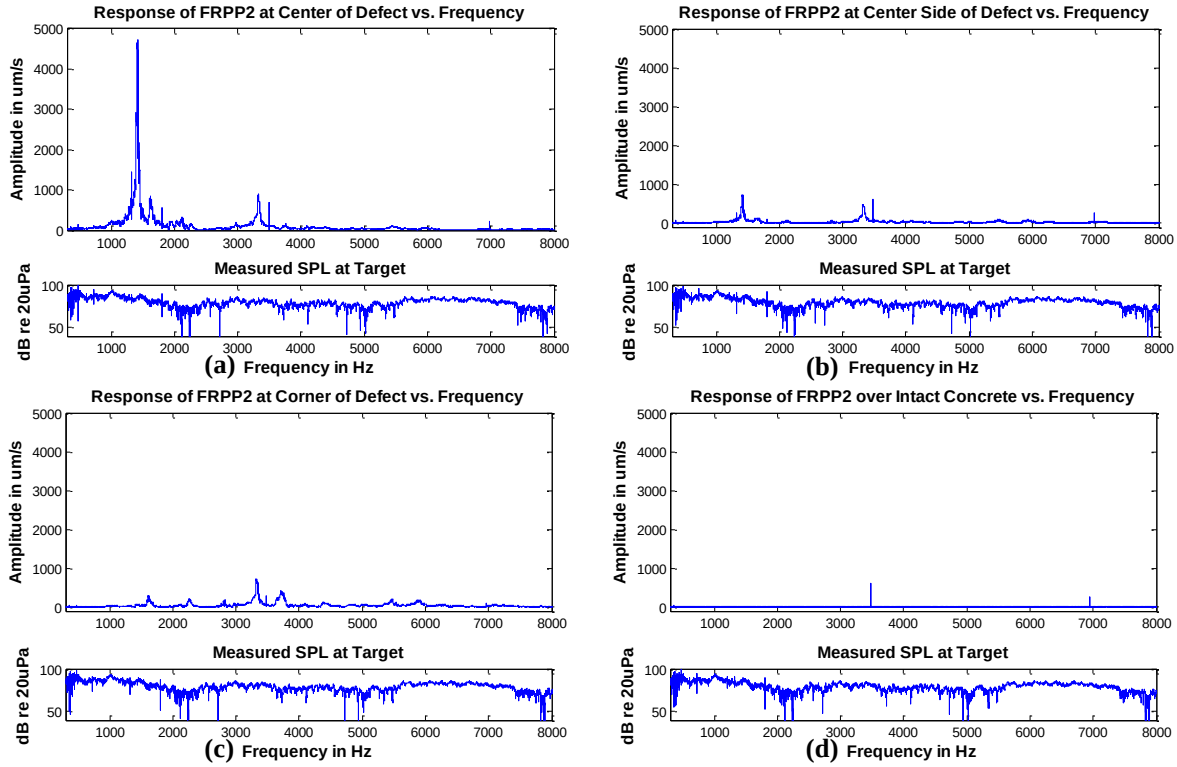

Figure 3: Response velocity spectrums of the specimen at the center of the defect (a), center side of the defect (b), corner of the defect (c), and over intact FRP-concrete system (d)

The base frequency observed of 1380 Hz in figure 3a is comparable to the estimated predicted resonant frequency of 1288 Hz from plate theory, when taking into consideration the possible variances in the material properties of the FRP. Our theory considers an isotropic material, while in practice, FRP is less stiff in the direction perpendicular to the fiber direction, resulting in lower resonant frequencies for the higher resonant modes. These plots also show that the response amplitude is much greater over the defect, with distinct resonant peaks of velocities ranging from 100 µm/s to upwards of 4500 µm/s. The measurement over intact concrete in Figure 3d shows only a noise floor of about 5 µm/s with some extraneous "hairs" due to noise. This large difference in vibration amplitude allows for identification of defective areas of the defect.

Image Construction

In order to determine the detectability capabilities of the system and physical modal structure of the defect, measurements were made in a 15 by 15 grid area encompassing the defect and the surrounding intact FRP. The defect is covered by the inner 11 by 11 grid area. A frequency sweep measurement was taken at each point and then the resonance peak vibration velocities were determined to make a plot of the vibration velocities at a given frequency in relation to their location on the specimen. Selected plots are shown in Figure 4, demonstrating the different vibrational modes that were captured with the grid measurements. These measurements show how the vibration amplitude varies for each vibrational mode and how it decreases near the defect boundaries and over intact concrete where no response is expected. The area surrounding the defect is deep blue, indicating low vibration amplitude, while colors indicating higher vibration amplitudes are over the defect. Clear modal lines can be seen in the measurements allowing us to identify distinct vibrational modes, such as the first resonant mode at 1380 Hz in Figure 4a, the 1580 Hz 2,1 mode in Figure 4b, the 2050 Hz 3,1 mode in Figure 4c, the 3260 Hz 1,3 mode in Figure 4d, the 3580 Hz 2,3 mode in Figure 4e, and the 3940 Hz 3,3 mode in Figure 4f.

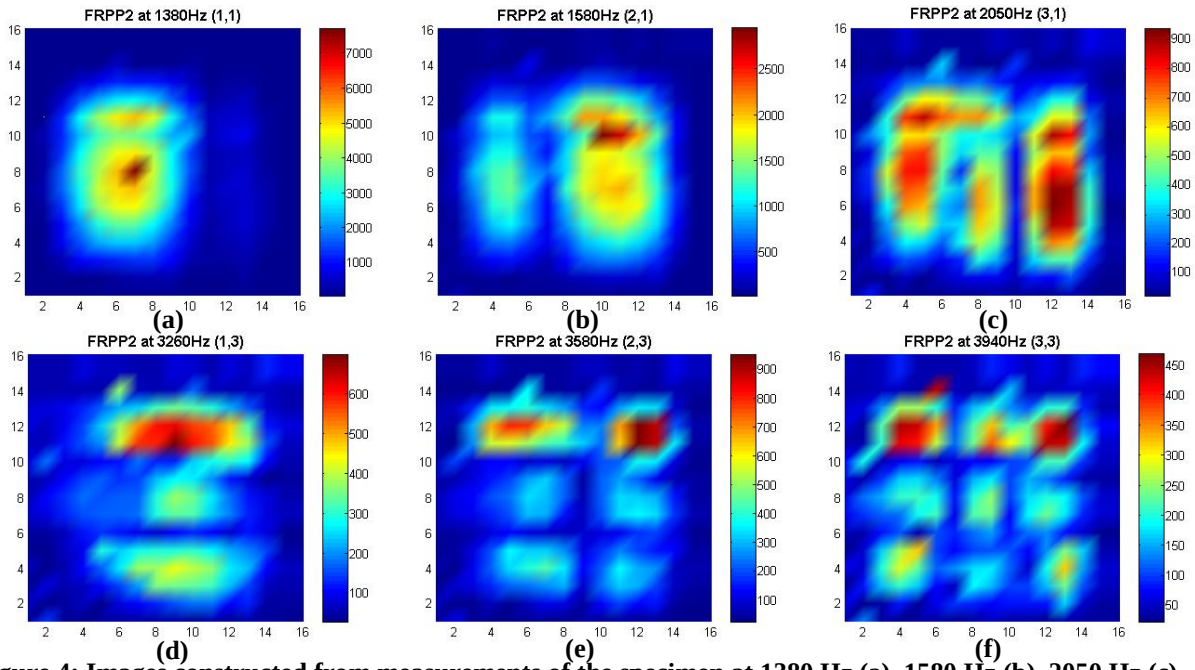

Figure 4: Images constructed from measurements of the specimen at 1380 Hz (a), 1580 Hz (b), 2050 Hz (c), 3260 Hz (d), 3580 Hz (e), and 3940 Hz (f)

ROC Curve

Using the image construction data sets, a preliminary analysis of the probabilistic performance of the acoustic-laser vibrometry method was conducted. The receiver operating characteristic (ROC) curve is a simple way to visualize the measures of detector performance, true positive rate and false positive rate as a function of some detection level parameter [15]. For the measurements a detection vibration level was specified, above which the measurement was classified as a positive detection of a defect, and below which the measurement was classified as a negative detection. Since it is known which measurements were actually made on the defect or competent material, true positives and false positives can be distinguished to determine the true positive and false positive rates. A true positive rate of one means that all measurements on a defect were correctly classified as detections, while a false positive rate of zero means that no measurements over intact material were incorrectly classified as detections. The ROC curve in Figure 5a shows that the system can achieve a 90% positive detection rate with a false positive rate of only 3.6%.

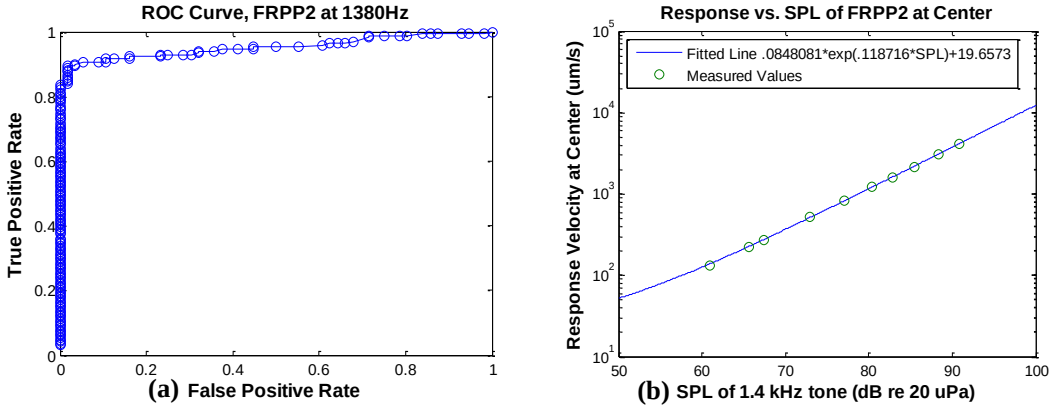

Figure 5: ROC curve for FRPP2 defect at 1380Hz (a) and response velocity vs. sound pressure level (b)

Parametric Studies

A series of parametric studies was conducted to help determine the feasibility of the method, varying parameters such as the sound pressure level, laser signal level, angle of incidence, dwell time, and defect size.

Sound Pressure Level

The sound pressure level (SPL) incident on the specimen is a measure of the pressure of the acoustic excitation which causes the response vibration. A measurement was made varying the SPL from approximately 60 dB to 90dB as shown in Figure 5b. The expected relationship where the response velocity increases by a factor of 10 for an increase in SPL of 20, which corresponds to an increase in the actual incident pressure by a factor of 10, was found.

Laser Signal Level

The return laser signal level is an important parameter that will determine the noise floor of the laser vibrometer system. When less power is reflected back from the specimen, either because of poor surface quality, or increase in distance that reduces the amount of light captured by the laser vibrometer lens, the noise floor will increase. Typically, to ensure ideal conditions, retroreflective tape is used on the specimen, which reflects almost all of the incident laser power back to the laser vibrometer lens. However for this measurement, in addition to the use of retroreflective tape, neutral density filters were placed in front of the lens to reduce the amount of laser power both transmitted and received.

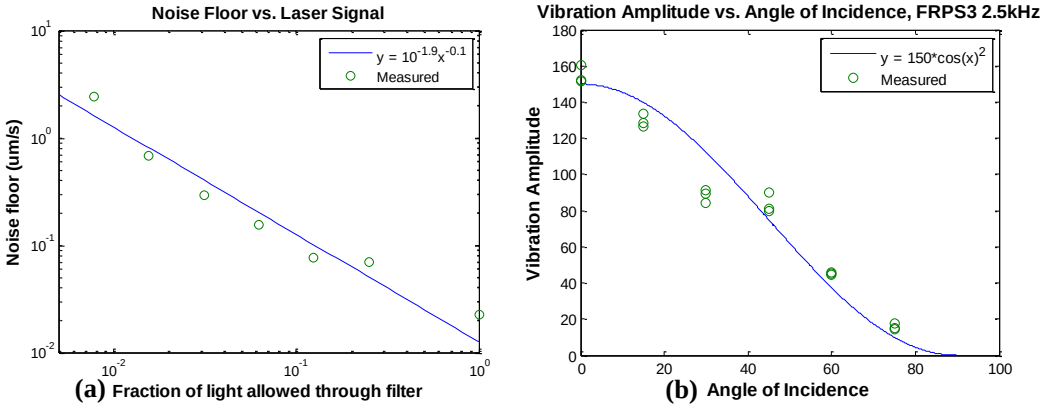

Figure 6: Noise floor vs. Laser attenuation (a) and vibration amplitude vs. angle of incidence (b)

From the plot in Figure 6a, for a factor of 10 reduction in the fraction of light received by the laser vibrometer, the noise floor also increases by a factor of 10. Since the amount of light reflected back into the laser vibrometer off of a lambertian surface follows an inverse square law, a factor of 10 reduction in the fraction of light corresponds to a square root of 10 (3.16) increase in distance from the specimen.

Angle of Incidence

The angle of incidence of the measurement system can greatly influence the measured response vibration amplitude. The laser vibrometer only measures movement collinear to the direction of the beam and the amount of power the acoustic excitation imparts to the specimen is greatest at normal incidence; both should follow a cosine dependence as the angle of incidence is changed. Therefore, for this measurement where the angle of the specimen is altered while the position of the laser vibrometer and speaker are fixed, a cosine squared dependence is expected.

Rippling of the surface of the FRP-P2 specimen made it impossible to make a consistent measurement of the effect of angle of incidence. In order to make an accurate measurement of the effect of angle of incidence, a different specimen, a prefabricated FRP plate epoxied to a steel plate, designated as "FRP-S3", was measured [16]. The flatness of the FRP surface allowed for measurement of the vibrational amplitude at angles of incidence: 0°, 15°, 30°, 45°, 60°, and 75°. Figure 6b shows the plot of the vibration amplitude measurements vs. the angle of incidence with an approximate cosine squared line superimposed over the data. The data followed the expected relationship.

Dwell Time

Dwell time is an important parameter because of the ability to improve the signal-to-noise ratio (SNR) with longer measurements, while a shorter measurement dwell time allows for quicker measurement coverage of an area. Two different acoustic excitations were used to study the effect of dwell time on the measurement. Since the data is fast Fourier transformed (FFT), a constant tone sine wave and a white noise waveform will excite the defect differently and change how the vibration signal peak integrates with time.

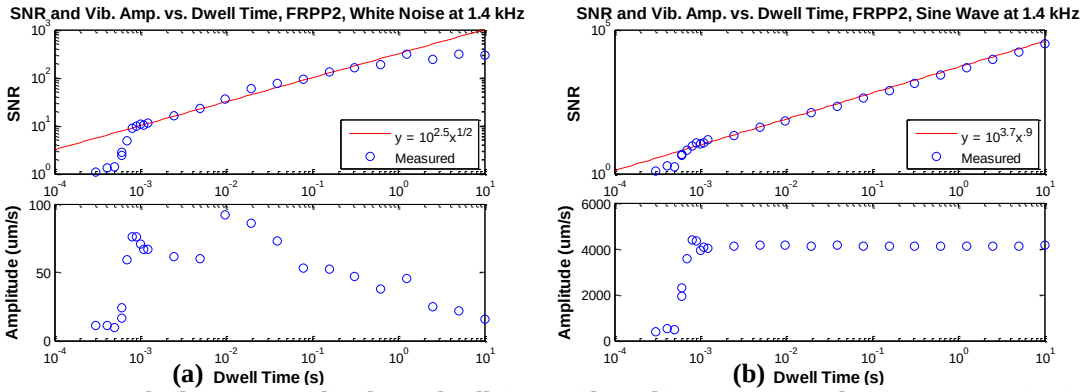

Figure 7: SNR and vibration amplitude vs. dwell time with a white noise (a) and a sine wave excitation (b)

A time of approximately 0.8 milliseconds is necessary to resolve the defect vibration, which corresponds to one cycle of vibration. As dwell time increased, SNR improved at different rates depending on the type of acoustic excitation. For the case of the constant sine wave excitation, when the dwell time increased by a factor of 10,000 from 1 millisecond to 10 seconds, the SNR improved by almost the same factor. With the white noise excitation, when the dwell time increased from 1 millisecond to 0.1 seconds, by a factor of 100, the SNR improved by a factor of only 10, because the amplitude decreased.

Defect Size

Another specimen was measured to investigate the effect of defect size. The prediction from plate theory is that if a defect were half the size, keeping boundary conditions and other physical properties the same, the first resonant frequency should increase by a factor of four. A second specimen designated as "FRP-P1" that consists of a similar concrete panel with bonded FRP, with a defect of size 1.5" by 1.5" by 1" deep, as seen in Figure 8a, was measured. Figure 8b shows a plot of the response velocity spectrum. The first resonant frequency of this defect was 3277 Hz which is about 2.4 times the larger defect's first resonant frequency of 1380 Hz. The reason for this inconsistency is that the FRP is directional and not isotropic, so the frequency did not increase by the theoretical factor of four.

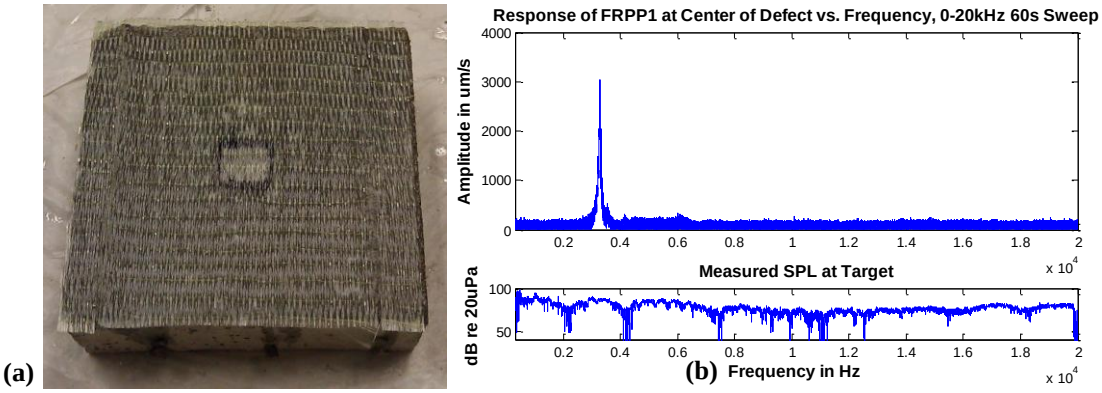

Figure 8: FRP-P1 specimen (a) and vibration response spectrum at the center of the defect (b)

CONCLUSIONS

The measurements show that the acoustic-laser vibrometry system is capable of detecting a delamination or void at the FRP-concrete interface in an FRP-retrofitted concrete system. In a laboratory environment, the acoustic-laser

vibrometry system provides a very large SNR for the detection of defects. This implies that even in less than ideal conditions when testing structures in the field, real defects should still exhibit enough response to be detected. Standoff capability of the system was demonstrated as the specimen was measured at a distance. Measurements under varying conditions were also conducted to determine the effects of sound pressure level, laser signal level, angle of incidence, dwell time, and defect size. The system shows great promise for being an effective methodology for the detection of defects at the FRP-concrete interface in FRP-retrofitted concrete with the potential for a new testing methodology in practice.

Future Work

Work for the future focuses on making the methodology closer to a field applicable technology. The data from the parametric studies can be used to estimate a probability of detection of a system under various conditions by altering the expected vibration amplitude or SNR. This will help inform the necessary specifications of an acoustic-laser vibrometry system for measurements in the field, where retroreflective tape is no longer required on the specimen by use of a more powerful, custom laser vibrometer.

ACKNOWLEDGMENTS

This research was supported by the National Science Foundation (NSF) CMMI Grant No. 0926671. The authors are grateful to the program managers, Dr. Mahendra Singh and Dr. Kishor Mehta for their interest in and support of this work. Special thanks to Tim Emge who helped with measurements and provided the specimen for the angle of incidence study. The authors would also like to thank MIT Lincoln Laboratory for providing experimental equipment and expertise.

REFERENCES

1. Meier, U. (1995), "Strengthening of structures using carbon fibre/epoxy composites," *Construction and Building Materials*, Vol. 9, No. 6. pp. 341-351.
2. Saadatmanesh, H., and M.R. Ehsani (1991), "RC beams strengthened with FRP plates. I: Experimental study," *Journal of Structural Engineering*, Vol. 117, No. 11, pp.3417-3433.
3. Buyukozturk, O., (1998), "Imaging of concrete structures," *NDT&E International*, Vol. 31, No. 4, pp. 233-243.
4. Yu, T.-Y. and O. Buyukozturk (2008), "A Far-field Airborne Radar NDT Technique for Debonding and Rebar Detection in GFRP-retrofitted Concrete Structures," *NDT&E International*, Vol. 41, pp.10-24.
5. Kachelmyer A.L. and K.I. Schultz (1995), "Laser vibration sensing," *Lincoln Laboratory Journal*, Vol. 8, No. 1, pp. 3-28.
6. Chen, F., and D. McKillip (2007), "Measurement and analysis of vibration and deformation using laser metrology for automotive applications," *Proc. IMechE, Part D: J. Automobile Eng*., Vol. 221, pp. 725-738.
7. Santulli, C., and G. Jeronimidis (2006), "Development of a method for nondestructive testing of fruits using scanning laser vibrometry (SLV)," *NDT.net*, Sep 2006, Vol. 11, No. 10.
8. Haupt R., and K.D. Rolt (2004), "Stand-off acoustic-laser technique to locate buried landmines," *Lincoln Laboratory Journal*, Vol. 15, No. 1, pp. 3-22.
9. Aranchuk, V., A. Lal, C. Hess, and J.M. Sabatier, "Multi-beam laser Doppler vibrometer for landmine detection," *Optical Engineering*, Vol. 45, 104302.
10. Beyer, S., D. Gornicki, and G. Muller (2004), "Analysis of laser-induced vibrations to detect non-adhesive regions of coatings," *Applied Physics A*, Vol. 79, pp. 1501-1504.
11. Ghoshal, A., A. Chattopadhyay, M.J. Schulz, R. Thornburgh, and K. Waldron (2003), "Experimental Investigation of Damage Detection in Composite Material Structures using a Laser Vibrometer and Piezoelectric Actuators," *Journal of Intelligent Material Systems and Structures*, Vol. 14, pp. 521-537.
12. Staszewski, W.J., B.C. Lee, L. Mallet, and F. Scarpa (2004), "Structural health monitoring using scanning laser vibrometry: I. Lamb wave sensing," *Smart Materials and Structures*, Vol. 13, pp. 251-260.
13. Leissa, A.W. (1969), *Vibration of Plates*, SP-160, NASA, US Government Printing Office, Washington, D.C.
14. Soedel, W. (2004), *Vibrations of Shells and Plates*, 3rd Ed., Marcel Dekker, New York, NJ.
15. Fawcett, T. (2006), "An introduction to ROC analysis," *Pattern Recognition Letters*, Vol. 27, Iss. 8, pp. 861-874.
16. Emge, T.J. (2012), *Remote Nondestructive Evaluation of Composite-Steel Interface by Acoustic Laser Vibrometry*, M.S. Thesis, Massachusetts Institute of Technology, Cambridge, MA.